Sixth International Symposium on Turbulence and Shear Flow Phenomena
Seoul, Korea, 22-24 June 2009

SIMULATION AND COMPARISON OF VARIABLE DENSITY ROUND AND PLANE JETS.

Holger Foysi
Aerodynamic Institute
RWTH Aachen, 52062 Aachen, Germany
h.foysi@aia.rwth-aachen.de

Juan P. Mellado
Institute for Combustion Technology
RWTH Aachen, 52062 Aachen, Germany
jmellado@itv.rwth-aachen.de

S. Sarkar
Department of Mechanical and Aerospace Engineering
UCSD San Diego, USA
ssarkar@ucsd.edu

ABSTRACT

Large-eddy simulations of plane and round variable density jets, as well as direct numerical simulations of plane jets were conducted using a variety of density ratios $s = \rho_j/\rho_{co}$, which relates the jet nozzle density ρ_j to the freestream density ρ_{co}. The initial momentum flux was kept constant for better comparison of the resulting data. Both simulations confirm experimental results, in that the jet half-width grows linearly with streamwise coordinate x and the lighter jets decay much faster than the heavy ones. The centerline velocity decay is however different between the plane and round geometries. Whereas the round jets exhibits a decay with $1/x$ for all density ratios, there seem to be two self-similar scalings in plane jets, in the limit of small and large density ratios. In the limit of small density ratios or incompressible flow, U_c scales as $U_c \sim 1/\sqrt{x}$, for strongly heated jets on the other hand we find $U_c \sim \sqrt{\rho_{co}/(x\rho_c)} \sim 1/x$. Using nondimensional values for x and U_c (Chen and Rodi [1980]) collapses the round jet data. Furthermore, the streamwise growth in mean density or the decay of the velocity fluctuations in the self-similar region is stronger for round jets. The round jet simulation with a density ratio of $s = 0.14$ shows additionally a global instability, whose frequency agrees excellently with experimental data.

INTRODUCTION

Variable density flows exhibit a range of interesting physical phenomena and arise in a variety of circumstances, e.g. during the mixing process between flows of different densities, during combustion processes or plasma processing. One phenomenon extensively studied in the past experimentally is the occurrence of global instabilities in variable-density jets (e.g. Monkewitz et al. [1990], Kyle and Sreenivasan [1993], Raynal et al. [1996], Hallberg and Strykowski [2006], Lesshaft et al. [2006]). However, a comparison of plane and round variable density jets and their different entrainment physics is lacking.
To the authors knowledge, there are only a few simulations available, which investigate variable density jets using LES (Zhou et al. [2001], Tyliszczak and Boguslawski [2006], Wang et al. [2008]) or DNS (Lesshaft et al. [2006]), 2D-DNS). However, there is no detailed investigation comparing plane and round jets at various density ratios $s = \rho_j/\rho_{co}$ (the subscript "j" indicates values at the virtual nozzle exit). Furthermore, a DNS database would be very valuable, since it would enable us to test LES and Reynolds averaged models and provide insight into important physical mechanisms. Another import aspect, as mentioned above, is the occurrence of global instabilities (Kyle and Sreenivasan [1993]), reported to occur if the ratio of the exiting nozzle fluid density to ambient fluid density is $\rho_j/\rho_{co} < 0.6$. Above that ratio, the shear-layer fluctuations evolve in a fashion similar to that observed in a constant-density jet, characterized by weak background disturbances. Below that threshold on the other hand, intense oscillatory instabilities may also arise. Since the oscillatory mode was shown to repeat itself with extreme regularity and is subject to strong vortex pairing, abnormally large velocity fluctuations were observed, requiring a large number of grid points. The overall behavior depends not only on the density ratio and the relation of the shear layer thickness to the nozzle width, but also on the Reynolds number (Hallberg and Strykowski [2006]).

DETAILS OF THE SIMULATIONS

The filtered compressible equations of motion are solved in cylindrical (r,θ,x) coordinates for the round jet using the compressible form of the dynamic Smagorinsky model (Martin et al. [2000]). Treatment of the centerline singularity at $r = 0$ is accomplished by using the centerline treatment according to Constantinescu and Lele [2002], where a series expansion is used for the equations at the centerline. For time integration a low-dispersion-dissipation Runge-Kutta scheme of (Hu et al. [1996]) in its low storage form is used. Spatial differentiation uses optimized DRP-SBP (dispersion-relation-preserving summation by parts) explicit finite-difference operators (Johansson [2004]). The code employed for the plane jet has been derived from Stanley et al.

Sixth International Symposium on Turbulence and Shear Flow Phenomena
Seoul, Korea, 22-24 June 2009

[2002], and is based on sixth-order compact Padé schemes for space derivatives and a Runge-Kutta fourth-order scheme for time advancement. Tables 1 and 2 give an overview over the different simulation parameters. The initial momentum

Case	Re	$D/\delta_{\theta 0}$	s	m_j
R014	7000	27	0.14	0.1
R100	21000	27	1.00	0.1
R152	32000	27	1.52	0.1
DNS PD050	1414	20	0.50	0.1
DNS PD100	2000	20	1.00	0.1
Plane jet LES	∞	10	0.125 - 1	0.1

Table 1: Parameters of the simulations ($Re = u_j \rho_j D/\mu_j$, initial momentum thickness $\delta_{\theta 0}$, initial dimensional momentum flux m_j, L_i normalized by r_j and D (slot width) for the round and plane jet, respectively). For the plane jet LES see Mellado [2004] for details.

Case	L_x	L_y	L_z	n_x	n_y	n_z
R014	60	2π	16	256	112	64
R100	60	2π	16	256	112	64
R152	60	2π	16	256	112	64
PD050	22	22	13	768	512	512
PD100	22	22	13	768	512	512
Plane jet LES	26	16	12	192	160	96

Table 2: Parameters of the simulations, L_i normalized by r_j or D (slot width) for the round and plane jet, respectively).

flux m_j has been fixed for all simulations. This reasoning was based on observations of Ricou and Spalding [1961], who showed that the entrainment rate of a jet strongly depends on m_j. Ruffin et al. [1994] demonstrated additionally, that the Taylor and Kolmogorov length scales are determined by the initial momentum flux. This reasoning was adopted, too, by other experiments and simulations, for example Amielh et al. [1996], Djeridane et al. [1996], Wang et al. [2008]. Non-reflecting boundary conditions (Lodato et al. [2008]) were applied, together with a combination of grid stretching and spatial filtering close to the boundaries. The round jet simulations were initialized using velocity profiles of the form (Bodony and Lele [2005])

$$u = u_{co} + \frac{1}{2}(u_j - u_{co})\left(1 - \tanh\left[\left(\frac{r}{r_j} - \frac{r_j}{r}\right)\frac{1}{4\delta_{\theta 0}}\right]\right),$$

and temperature fields using the Crocco-Busemann relation. For the plane jet similar profiles were applied (replace r_j with $D/2$ and r with y), making use of the symmetry at $y = 0$. To trigger the transition to turbulence precursor simulations of annular and plane temporally evolving mixing layers with smaller initial momentum thickness were performed for the round and plane jet problem, respectively. The square root of the turbulent kinetic energy was monitored until its non-dimensional value $\sqrt{(u')_1^2 + (u')_2^2 + (u')_3^2}$ was of the order of 0.05 and the mean velocity profiles agreed closely with the prescribed inlet mean jet profiles. The resulting fluctuations were convected into the fluid domain using the characteristic inflow boundary conditions. Figures 1 and 2 show contour plots of the density for simulation R014 and P05, respectively, for illustration of the jet development.

RESULTS

Figure 3 shows the mean velocity difference $\Delta U = \bar{U} - U_{co}$ normalized by the centerline velocity at various streamwise positions for cases R014 and R100. All profiles for the round jet collapse nicely, indicating self-similar behavior. They furthermore agree well with an exponential of the form $u = \exp[-(r/r_j)^2 \ln 2]$. For the plane jet, too, we observe a collapse of the streamwise velocity difference at various x-locations and for different density ratios (figure 4). The decay of the centerline velocity U_c of variable density jets has been investigated by many researches, before. No *general* similarity solution may be found for plane jets, as pointed out by Mellado [2004]. For incompressible flow and low density ratios dimensional analysis and conservation of momentum suggests that $U_c/U_j \sim \sqrt{hs/x}$. Figure 5, which shows the centerline velocity decay for the plane jet LES simulations, confirms this relationship. We furthermore see that lighter jets decay much faster than heavy jets, owing to the conservation of streamwise momentum. For high s, however, density itself scales with $\rho_c/\rho_j \sim x/D$, leading to $U_c/U_j \sim h/x$. A mixed scaling was proposed by Mellado [2004] to cover both limits, using the centerline density ρ_c instead of ρ_j, giving $U_c/U_j \sim \sqrt{h\rho_{co}/(\rho_c x)}$. This scaling collapses the profiles for the plane jet as shown in figure 6. Such a simple scaling didn't work for the round jet case, whose centerline velocity decay is shown in figure 7. Here, the Witze scaling (Witze [1974]) is used to obtain a common potential core collapse location $x_c/r_0 = 0.7[\kappa^2/s]^{-1/2}$ where $\kappa = 0.08(1 - 0.16M_j)s^{-0.22}$. The simulations are compared with data from (Crow and Champagne [1971], Bridges and Wernet [2003], Bodony and Lele [2005]) at $s = 0.95$ (Bridges and Wernet [2003], Bodony and Lele [2005]) and $s = 1$ (incompressible Crow and Champagne [1971]). The observed linear growth of $1/U_c$ with x agrees with the prediction of self-similar analysis (So [1986]), although several assumptions are made, including that of a constant Chapman-Rubesin parameter. A better collapse of the data is obtained by using the analysis of Chen and Rodi [1980], expressing the velocity decay using a nondimensional downstream distance parameter $x^* = s^{-1/4}x$ and centerline velocity $U_c^* = s^{-1/4}U_c/U_{co}$, as is seen in figure 8.

The development of the centerline density is seen in figure 9, for the round jet case with $s = 1/7$ and the plane jet cases with $s = 0.8, 1/8$. Both, plane and round jets, first show only minor mixing before nonlinear growth occurs. As reported by Mellado [2004], after this nonlinear growth phase the jet density continues to increase almost linearly for case $s = 1/8$. Self-similar analysis predicts this mean density linear regime for strongly heated jets, before the core density reaches values comparable to the co-flow; beyond that point, temperature becomes a passive scalar if no buoyancy is present. The round jet centerline density grows faster, but starts to increase slightly further downstream than the plane jet simulations. This seems to be caused by the strong global instability, to be discussed below, and slightly different initial conditions. The stronger growth in simulation R014 compared to the plane jet simulations could be expected, however, due to the larger surface undergoing turbulent mixing relative to the plane jet.

Contrary to the centerline velocity decay, the jet half width (position at which the streamwise velocity dropped to half the centerline value) grows linearly in x (figure 10 and 11). The half width for plane and round jet was, irrespective of the density ratio,of similar magnitude, 0.112 vs. 0.116, respectively. The round jet data is compared with a simulation from Bodony and Lele [2005] at $s = 0.95$, the plane jet data with experiments from Browne et al. [1983], Ramaprian and Chandrasekhara [1985]. When shifted by the virtual origin x_s it can be seen that the growth rate is the same within the round or plane jet data, irrespective of the density ratio s. Figure 12 shows a comparison of the evolution of the Reynolds stress components in radial direction for the round jet and cross-stream direction for the plane jet (other components show similar trends). Interestingly, the peak values are of the same order of magnitude. With increasing density ratio higher fluctuation levels are observed, consistent with results from Djeridane et al. [1996]. The initial growth for the round jet cases is different, but it is possible, by using the Witze scaling, collapse the profiles in the early development region. As observed for the mean density growth, during the self similar stage a different evolution of round and plane jets is obvious here, too. The peak is more pronounced for the round jet simulations, with a stronger decrease thereafter.

In Case R014, high amplitude oscillations were observed, especially for the streamwise velocity and density, leading to strong gradients which made the simulation unstable at first. Adding artificial dissipation (Fiorina and Lele [2007]) helped stabilizing the calculation. This strong oscillating mode together with the strong vortex pairing events as well as the occurrence of side jet phenomena points toward the existence of a global instability in this simulation. Evidence for this is shown in figure 13, plotting the power spectrum of the streamwise velocity at various streamwise locations. The power spectrum clearly shows the fundamental frequency and its sub-harmonics at various streamwise positions (shifted for better visibility). The peak is clearly visible until a sudden transition to turbulence has occurred around $x/D = 7$. The Strouhal number of this oscillating mode $St_D = fD/U_j$ was calculated and compared to various experimental datasets, depicted in figure 14. Excellent agreement is seen between the simulation results and the experimental data. For the plane jet simulations no such global mode was observed, neither in the DNS nor the LES simulations. After Hallberg and Strykowski [2006], the global oscillations depend on the density ratio s, $D/\delta_{\theta 0}$ and the Reynolds number, as long as compressibility and buoyancy effects are unimportant. Going further than Kyle and Sreenivasan [1993], Hallberg and Strykowski [2006] nondimensionalize the frequency by the *viscous* time scale D^2/ν, thus retaining the Reynolds number in the frequency dependence. They were then able to collapse all data onto a straight line, when plotting fD^2/ν over $Re\sqrt{D/\delta_{\theta 0}}(1+\sqrt{s})$. Having similar initial momentum thickness and density ratio and higher Re than required for the occurrence of global modes at a given momentum thickness in the plane jet cases (Hallberg and Strykowski [2006]) a possible reason might be the plane jet geometry itself or the different Mach number. Simulations at various Mach numbers are performed currently, to answer this question.

CONCLUSIONS

Results of DNS simulations of plane jets and LES simulations of round and plane jets at various density ratios, ranging from $s = 0.125$ to $s = 1.52$ have been presented in the text. The streamwise linear growth of the round and plane jet half width was found to be of similar magnitude, with slightly lower growth of the round jets and independent of the density ratio, a fact reported in the literature before. The centerline velocity decay rates are strongly affected by heating and exhibit different behavior for round and plane jets. Whereas the round jets exhibits a decay with $1/x$ for all density ratios, there are two self-similar scalings found in plane jets, in the limit of small and large density ratios. In the limit of small density ratios or incompressible flow, U_c scales as $U_c \sim 1/\sqrt{x}$, for strongly heated jets on the other hand we find $U_c \sim \sqrt{\rho_{co}/(x\rho_c)} \sim 1/x$, which is due to a linear growth of the centerline density. Using nondimensional values for x and U_c (basically scaling the quantities using the factor $s^{-1/4}$ after Chen and Rodi [1980]) collapses the round jet data. This clearly shows a difference in the development and entrainment process of round and plane jets, which should be considered when developing RANS models. Furthermore, it was seen that the streamwise growth in mean density or the decay of the velocity fluctuations in the self-similar region, after the transition region, is stronger for round jets. The core density reached co-flow values much faster for the round jet and therefore the interval of distances x in which there is a strong density difference between the core and the co-flow is shortened, and it is more difficult to find an intermediate self-similar regime. We believe, that further insight might be found in analyzing the vorticity development and enstrophy budget for both geometries. This, however, requires DNS simulations of the round jet, currently performed on 1024 processors at the Julich supercomputing center, in order to resolve the small scales appropriately, necessary to reliably interpret the enstrophy budget.
The round jet data at $s = 0.14$ furthermore shows a global instability, with the fundamental frequency in excellent agreement with previous experimental data, as summarized by Hallberg and Strykowski [2006]. Such a global mode couldn't be seen in the plane jet simulations, probably due to the different Mach numbers. This, however, is ongoing research.

*

References

M. Amielh, T. Djeridane, F. Anselmet, and L. Fulachier. Velocity near-field of variable density turbulent jets. *Int. J. Heat Mass Transfer*, 39(10):2149–2164, 1996.

D. Bodony and S. Lele. On using large-eddy simulation for the prediction of noise from cold and heated turbuent jets. *Physics of Fluids*, 17(8):85–103, 2005.

J. Bridges and M.P. Wernet. Measurements of the aeroacoustic sound source in hot jets. *AIAA Pap. 2003-3130*, 2003.

L. W. B. Browne, R. A. Antonia, S. Rajagopalan, and A. J. Chambers. Structure of complex turbulent shear flows. pages 411–419, 1983.

C.J.. Chen and W. Rodi. Vertical Turbulent Buoyant Jets: a Review of Experimental Data. *Pergamon Press, Great Britain*, 1980.

G. Constantinescu and S. K. Lele. A highly accurate technique for the treatment of flow equations at the polar axis in cylindrical coordinates using series expansions. *J. Comp. Phys.*, 183(1):165–186, 2002.

S.C. Crow and F.H. Champagne. Orderly structure in jet turbulence. *J. Fluid Mech.*, 48:547, 1971.

T. Djeridane, M. Amielh, F. Anselmet, and L. Fulachier. Velocity turbulence properties in the near-field region of variable density jets. *Phys. Fluids*, 8(6):1614–, 1996.

B. Fiorina and S. K. Lele. An artificial nonlinear diffusivity method for supersonic reacting flows with shocks. *J. Comp. Phys.*, 222(1):246–246, 2007.

M.P. Hallberg and P.J. Strykowski. On the universality of global modes in low-density axisymmetric jets. *J. Fluid Mech.*, 569:493–, 2006.

F.Q. Hu, M.Y. Hussaini, and J.L. Manthey. Low-dissipation and lowdispersion rungekutta schemes for computational acoustics. *J. Comput. Phys.*, 124:177–197, 1996.

Stefan Johansson. High order finite difference operators with the summation by parts property based on DRP schemes. Technical Report 2004-036, it, August 2004.

D.M. Kyle and K.R. Sreenivasan. The instability and breakdown of a round jet variable-density jet. *J. Fluid Mech.*, 249:619–664, 1993.

L. Lesshaft, P. Huerre, P. Sagaut, and M. Terracol. Nonlinear global modes in hot jets. *J. Fluid Mech.*, 554:393–, 2006.

Guido Lodato, Pascale Domingo, and Luc Vervisch. Three-dimensional boundary conditions for direct and large-eddy simulation of compressible viscous flows. *Journal of Computational Physics*, 227(10):5105 – 5143, 2008.

M.P. Martin, U. Piomelli, and G.V. Candler. Subgrid-scale models for compressible large-eddy simulations. *Theoret. Comp. Fluid Dyn.*, 13:361–376, 2000.

J. P. Mellado. Large-eddy simulation of variable density flows. *PH.D Thesis, UCSD San Diego*, 2004.

P.A. Monkewitz, D.W. Bechert, B. Barsikow, and B. Lehmann. Self-excited oscillations and mixing in a heated round jet. *J. Fluid Mech.*, 213:611, 1990.

B. R. Ramaprian and M. S. Chandrasekhara. Lda measurements in plane turbulent jets. *Trans. ASME: J. Fluids Engng*, 107:264–271, 1985.

L. Raynal, J.-L. Harion, M. Favre-Marinet, and G. Binder. The oscillatory instability of plane variable-density jets. *Phys. Fluids*, 8:993, 1996.

F.P. Ricou and D.B. Spalding. Measurements of entrainment by axisymmetrical turbulent jets. *J. Fluid Mech.*, 11:21, 1961.

E. Ruffin, R. Schiestel, F. Anselmet, M. Amielh, and L. Fulachier. Investigation of characteristic scales in variable density turbulent jets using a second-order model. *Physics of Fluids*, 6(8):2785–2799, 1994. doi: 10.1063/1.868167.

R.M.C. So. On self-preserving, variable-density, turbulent free jets. *J. Appl. Math. and Phys.*, 37:538–558, 1986.

S. A. Stanley, S. Sarkar, and J. P. Mellado. A study of the flowfield evolution and mixing in a planar turbulent jet using direct numerical simulation. *J. Fluid Mech.*, 450: 377–407, 2002.

Tyliszczak and Boguslawski. Les of the jet in low mach variable density conditions. *Direct and Large-Eddy Simulation VI, Part XII*, page 575582, 2006.

P. Wang, J. Fröhlich, V. Michelassi, and W. Rodi. Velocity near-field of variable density turbulent jets. *Int. J. Heat Fluid Flow*, 29:654–664, 2008.

P.O. Witze. Centerline velocity decay for compressible free jets. *AIAA J.*, 12:417, 1974.

X. Zhou, K.H Luo, and J.J.R. Williams. Study of density effects in turbulent buoyant jets using large-eddy simulation. *Theor. Comput. Fluid Dyn.*, 15:95120, 2001.

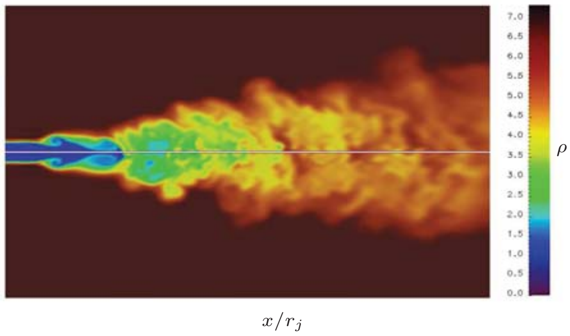

Figure 1: Contour plot of the density for case R014.

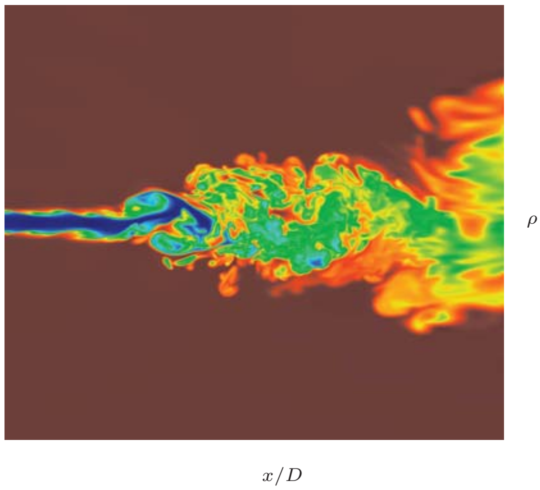

Figure 2: Contour plot of the density for case P05. Color table similar to figure 1.

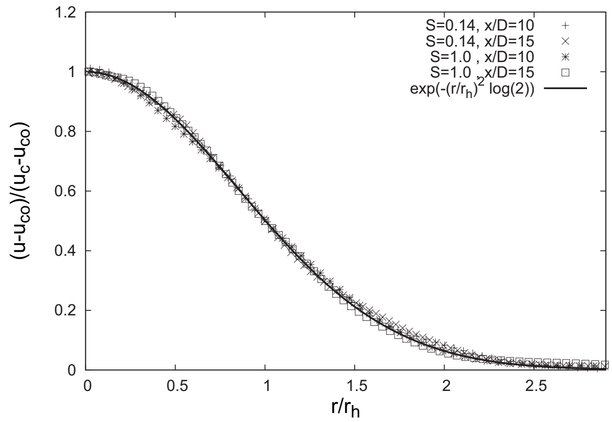

Figure 3: Normalized velocity difference at various streamwise positions for the round jet LES, normalized by the jet half width.

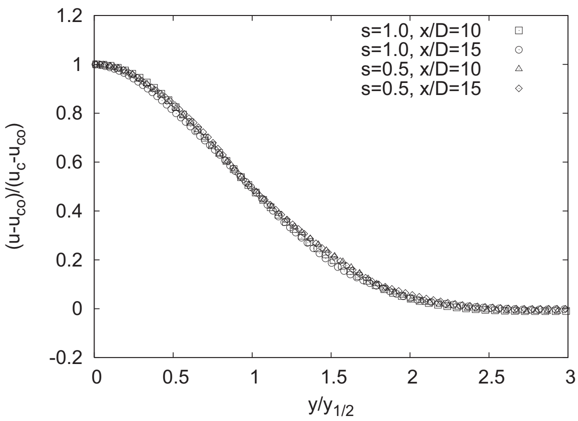

Figure 4: Normalized velocity difference at various streamwise positions for the DNS of the plane jet normalized by the jet half width.

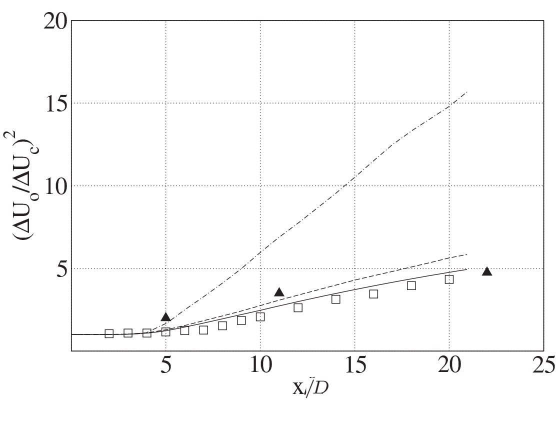

Figure 5: Centerline velocity decay for the plane jet LES results. ——— $s = 1$, $- - - s = 0.8$, $-. - .s = 1/8$, □ Browne et al. [1983] and ▲ Ramaprian and Chandrasekhara [1985].

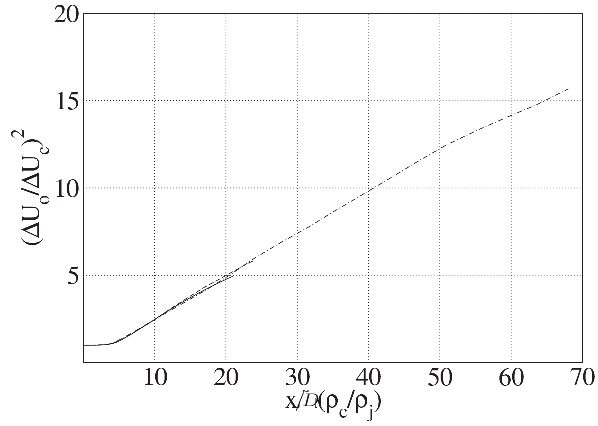

Figure 6: Centerline velocity decay for the plane jet LES results, using the centerline density. ——— $s = 1$, $- - - s = 0.8$, $-. - .s = 1/8$.

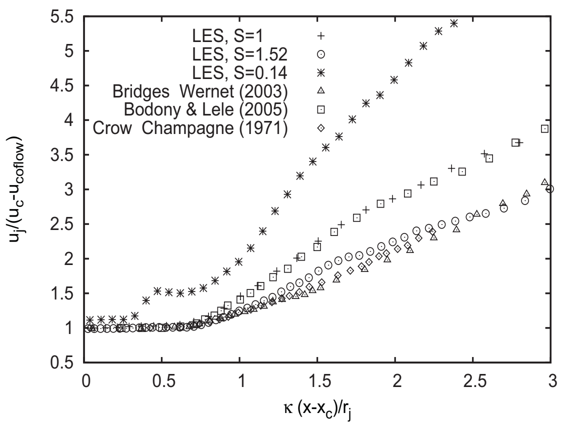

Figure 7: Centerline streamwise velocity decay of the round jet using the Witze scaling (Witze [1974]).

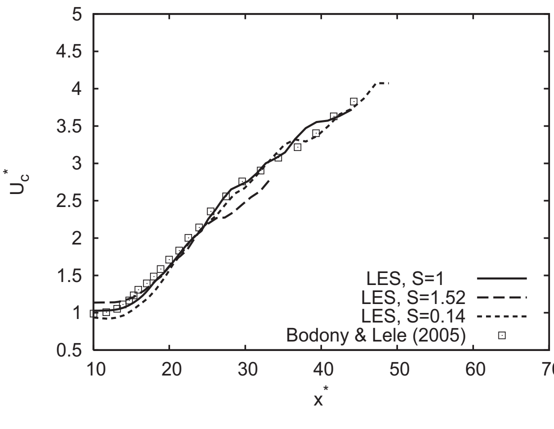

Figure 8: Centerline velocity decay using $U_c^* = s^{-1/4} U_c/U_{co}$ and $x^* = s^{-1/4}(x - x_s)$. The streamwise coordinate was shifted using the virtual origin x_s.

Sixth International Symposium on Turbulence and Shear Flow Phenomena
Seoul, Korea, 22-24 June 2009

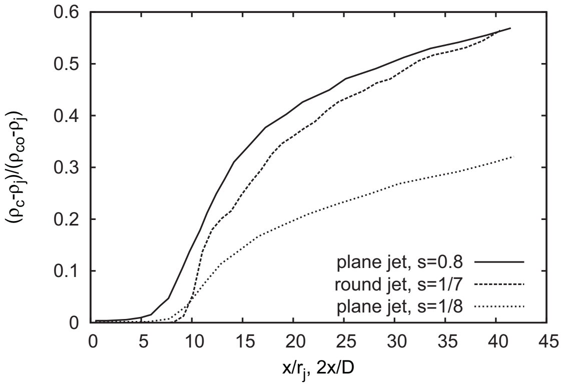

Figure 9: Growth of centerline density $(\rho_c - \rho_j)/(\rho_{co} - \rho_j)$ for case R014, compared to the plane jet LES cases with $s = 1/8$ and $s = 0.8$. h is the slot width.

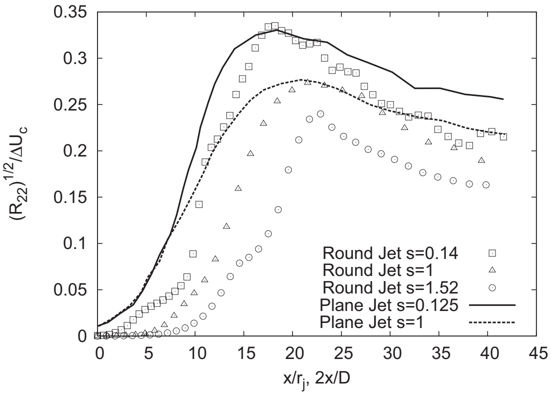

Figure 12: Streamwise evolution of the centerline cross-stream Reynolds stress normalized using the centerline velocity difference, taken from the LES results.

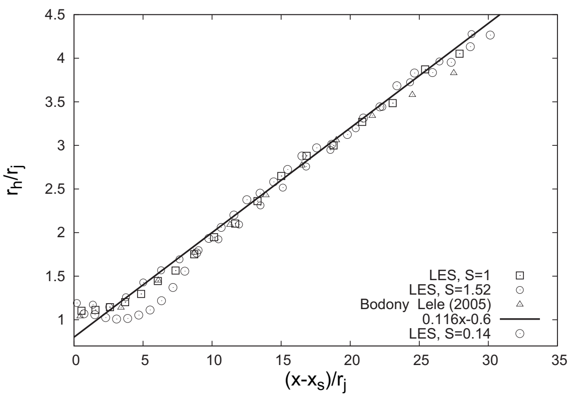

Figure 10: Streamwise evolution of the velocity half-width of the round-jet LES, shifted by using the virtual origin x_s.

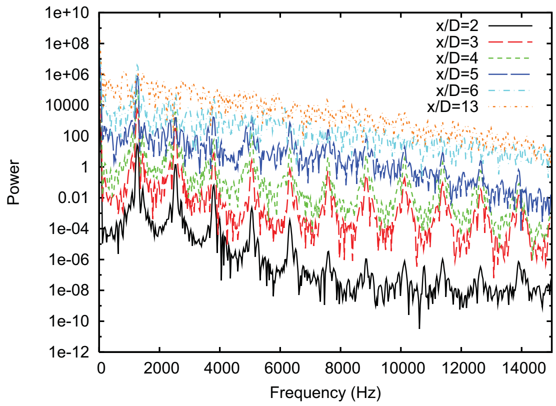

Figure 13: Frequency power spectrum of u_x at various streamwise positions (curves shifted for better visibility).

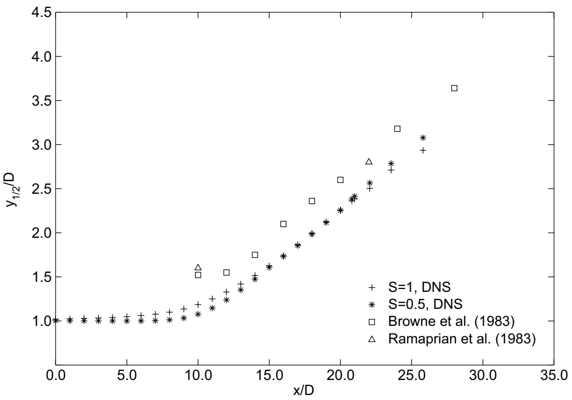

Figure 11: Streamwise evolution of the velocity half-width of the plane-jet DNS.

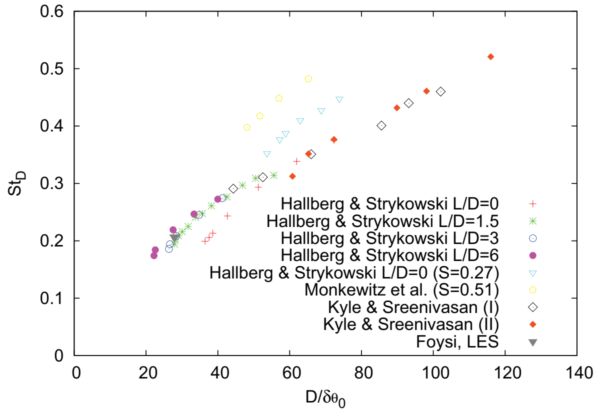

Figure 14: Strouhal number of the global instability mode, compared with experimental data.